ARTICLE

Förster Resonance Energy Transfer in Fluorophore Labeled Poly(2-ethyl-2-oxazoline)s

Received 00th January 20xx,
Accepted 00th January 20xx

DOI: 10.1039/x0xx00000x

Ronald Merckx[a], Thomas Swift[b], Ryan Rees[b], Joachim F. R. Van Guyse[a], Ella Schoolaert[c], Karen De Clerck[c], Heidi Ottevaere[d], Hugo Thienpont[d], Valentin Victor Jerca[a],[e*], Richard Hoogenboom[a*]

Dye-functionalized polymers have been extensively studied to understand polymer chain dynamics, intra or inter-molecular association and conformational changes as well as in practical applications such as signal amplification in diagnostic tests and light-harvesting antennas. In this work, the Förster resonance energy transfer (FRET) of dye-functionalized poly(2-ethyl-2-oxazoline) (PEtOx) was studied to evaluate the effect of dye positioning and polymer chain length on the FRET efficiency. Therefore, both α- or ω-fluorophore single labeled as well as dual α, ω-fluorescent dye labeled PEtOx were prepared via cationic ring opening polymerization (CROP) using 1-(bromomethyl)pyrene as initiator and/or 1-pyrenebutyric acid or coumarin 343 as terminating agent, yielding well-defined PEtOx with high labeling efficiency (over 91 %). Fluorescence studies revealed that the intramolecular FRET is most efficient for heterotelechelic PEtOx containing both the pyrene and coumarin 343 fluorophores as chain ends, as expected. A strong dependence of the energy transfer on the chain length was found for these dual labeled polymers. The polymers were tested in both dilute organic (chloroform) and aqueous media revealing a higher FRET efficiency in water due to the enhanced emissive properties of the pyrene. The application of dual labeled polymers as fluorescent probes for temperature sensing was demonstrated based on the lower critical solution temperature behavior of the PEtOx. Furthermore, these polymers could be successfully processed into fibers and thin films. Importantly, the fluorescence properties were retained in the solid state without decreasing the FRET efficiency, thus opening future possibilities for application of these materials in solar cells and/or sensors.

Förster Resonance Energy Transfer in Fluorophore Labeled Poly(2-ethyl-2-oxazoline)s

Ronald Merckx[a], Thomas Swift[b], Ryan Rees[b], Joachim F. R. Van Guyse[a], Ella Schoolaert[c], Karen De Clerck[c], Heidi Ottevaere[d], Hugo Thienpont[d], Valentin Victor Jerca[a],[e*], Richard Hoogenboom[a*]

Dye-functionalized polymers have been extensively studied to understand polymer chain dynamics, intra or inter-molecular association and conformational changes as well as in practical applications such as signal amplification in diagnostic tests and light-harvesting antennas. In this work, the Förster resonance energy transfer (FRET) of dye-functionalized poly(2-ethyl-2-oxazoline) (PEtOx) was studied to evaluate the effect of dye positioning and polymer chain length on the FRET efficiency. Therefore, both α- or ω-fluorophore single labeled as well as dual α, ω-

Introduction

Dye-functionalized polymers have been extensively studied for their use in various fields such as nonlinear optics[1, 2], optical imaging[3, 4], light harvesting[5], optical sensor[6, 7], data storage[8, 9] and so on.[10, 11] Among them polymers that are end-functionalized with dyes have shown great promise in both theoretical areas for studying polymer chain dynamics, intra or inter-molecular association and conformational changes as well as in practical applications such as signal amplification in diagnostic test and light-harvesting antennas.[12-14] Förster Resonance Energy Transfer (FRET) is a very useful tool for the investigation of conformation transitions of a polymer chain and, thus, various sensors detecting the variation in the

[a] Supramolecular Chemistry Group, Centre of Macromolecular Chemistry (CMaC), Department of Organic and Macromolecular Chemistry, Ghent University, Krijgslaan 281-S4, 9000 Ghent, Belgium. E-mail: richard.hoogenboom@ugent.be
[b] Polymer and Biomaterials Chemistry Laboratories, School of Chemistry and Biosciences, University of Bradford, Bradford BD7 1DP, UK
[c] Centre for Textile Science and Engineering, Department of Materials, Textiles and Chemical Technology, Ghent University, Tech Lane Science Park 70A, 9052 Ghent, Belgium
[d] Brussels Photonics (B-PHOT) – Department of Applied Physics and Photonics, Vrije Universiteit Brussel, Pleinlaan 2, 1050 Brussels, Belgium
[e] Centre of Organic Chemistry "Costin D. Nenitzescu" Romanian Academy, Spl. Independentei 202B, 060023, Bucharest, Romania. E-mail: victor_jerca@yahoo.com

Electronic Supplementary Information (ESI) available: [details of any supplementary information available should be included here]. See DOI: 10.1039/x0xx00000x

molecular environment can be constructed based on the judicious choice of the FRET pair of fluorophores.[15-18] The FRET method has been extensively used in bio-related systems such as peptides, DNA, and proteins to obtain quantitative conformational information.[19-23] Moreover, the FRET technique was also used to study polymer functionality, architecture, colloidal properties and molecular weight.[24-31] Furthermore, the FRET probes are superior to single dye labeled probes due to their reduced sensitivity to concentration effects and possibility to monitor the process using two different wavelengths (i.e., ratiometric detection) which reduces the influence of different environmental parameters such as viscosity, pH, or polarity, thus allowing more accurate measurements. FRET analysis of α, ω-dye labeled synthetic polymers obtained by conventional radical polymerization offers only limited qualitative information due to the low labeling efficiency, complicated end-to-end distance distributions and artificial diffusion enhancement. Although well-defined heterotelechelic dye labeled polymers have been successfully obtained by means of controlled radical polymerization methods, their synthesis still remains laborious and involves several post-polymerization modification steps, generally resulting in low labeling efficiency.[15, 16, 32-34] Consequently, finding and developing new strategies to overcome the above-mentioned drawbacks represents the focus of the ongoing research.

Poly(2-alkyl/aryl-2-oxazoline)s (PAOx) are a synthetic class of polyamides, that are obtained by living cationic ring-opening polymerization (CROP) of 2-oxazoline monomers.[35-41] The polymers are characterized by narrow molecular weight distributions, and various functional groups can be easily introduced at the α- and ω-chain ends through both initiation and termination, respectively.[39] In the past decade, PAOx have become of particular interest as versatile biomaterials, with poly(2-ethyl-2-oxazoline) (PEtOx) being the most frequently studied member of this class.[42-46] Moreover PAOx have also been successfully used in the construction of solar cells, materials with multicolor emission and thermoresponsive photoluminescent materials.[47-51] Therefore, single-labeled polymers have conveniently been synthesized using either terminator or "initiator method". Even though combining both methods would enable facile access to α, ω-dual labeled polymers, this has not yet been explored to study the FRET behavior of such polymers, to the best of our knowledge. The fluorophores must be adequately chosen to provide the correct and desired information about the investigated system. The fluorophores should have high molar extinction coefficients and quantum yields as well as good photostability. In addition, an optimal FRET pair should have: i) large spectral separation between donor and acceptor emission, and ii) similar quantum yields and detection efficiencies. Consequently, in this work we focused our attention to pyrene and coumarin 343 as the FRET donor and acceptor, respectively. Previous reports have demonstrated that this fluorophore pair can be used for intramolecular FRET in peptides, and in synthetic polymer systems,[52, 53] making it an ideal system to study the effect of fluorophore positioning in dye-functionalized PEtOx.

Thus, in the present study we demonstrate that the living CROP of 2-ethyl-2-oxazoline allows facile access to single and/or dual labeled polymers. These polymers serve as basis to study the effect of dyes-positioning as well as polymer chain length on the FRET efficiency in different solvents. Finally, the applicability of these systems as FRET-based solution temperature sensors as well as for solid state applications based on energy transfer between the FRET dyes in thin films and nanofibers was assessed. The current study not only expands the synthetic methodologies to obtain well-defined heterotelechelic polymers by CROP but also paves the way to future applications for *in vivo* imaging and/or *in vitro* assay studies that are highly needed not only for PAOx homopolymers but also copolymers in the quest of moving forward towards advanced *in vivo* applications. Moreover, the optimized labelling protocol developed in this study could be easily transferred to amphiphilic PAOx block-copolymers, which are demonstrated to be promising candidates for the construction of drug delivery systems[54-57] to obtain important information regarding the exchange dynamics which is difficult to acquire using other methods.

Experimental section

Materials

All the common used solvents were HPLC grade and include: dichloromethane (DCM, >99.8%, Sigma Aldrich), diethyl ether (>99.9%, Sigma Aldrich), acetonitrile (ACN, >99.9%, Sigma Aldrich), chloroform ($CHCl_3$, >99%, Fisher Chemical) and N,N-dimethyl formamide (DMF, >99%, Biosolve). Dry DCM, triethylamine (TEA, ≥99.5%, Sigma Aldrich), tetrahydrofuran (THF, ≥99.9%, Sigma Aldrich) and ACN were obtained from a custom made J.W. Meyer solvent purification system and were dried over alumina oxide columns. The following chemicals were used as received: 1-pyrenebutyric acid (>98.0%, TCI), extra dry chlorobenzene (>99%, Acros Organics) and the coumarin 343 (>97.0%, TCI). 2-Ethyl-2-oxazoline was kindly donated by Polymer Chemistry Innovations and purified by fractional distillation over barium oxide (>90%, Acros Organics) and ninhydrin (ACS reagent, Sigma-Aldrich) under Argon atmosphere. Methyl p-toluenesulfonate (≥98%, Sigma Aldrich), used as initiator in the polymerizations, was distilled over BaO under argon atmosphere to remove traces of water. 1-(bromomethyl)pyrene (>92.0%, Sigma Aldrich) was recrystallized from $CHCl_3$ (3 times). Following products were used as received: sodium bicarbonate (≥99.7%, Sigma-Aldrich), magnesium sulfate (≥99.5%, Sigma Aldrich), sodium chloride (>99%, Sigma-Aldrich) and potassium hydroxide (≥85.0%, Fisher-scientific). The PEtOx used for electrospinning was synthesized within our own group with following specifications Mn: 70 kDa; Mp: 85 kDa and Đ: 1.39.

Instrumentation

^{1}H-NMR spectra were recorded on a Bruker Avance 300 MHz at room temperature in chloroform-d ($CDCl_3$) purchased from Euriso-top. The chemical shifts are given in parts per million (δ), relative to $CDCl_3$ at 7.24 ppm.

Gas chromatography was performed on an Agilent 7890A system equipped with a VWR Carrier-160 hydrogen generator and an Agilent HP-5 column of 30 m length and 0.320 mm diameter. An FID detector was used and the inlet was set to 250 °C with a split injection of ratio 25:1. Hydrogen was used as carrier gas at a flow rate of 2 mL/min. The oven temperature was increased with 20°C/min from 50°C to 120°C, followed by a ramp of 50 °C/min to 300 °C.

Size exclusion Chromatography (SEC) Size-exclusion chromatography (SEC) was performed on a Agilent 1260-series HPLC system equipped with a 1260 online degasser, a 1260 ISO-pump, a 1260 automatic liquid sampler (ALS), a thermostatted column compartment (TCC) at 50 °C equipped with two PLgel 5 µm mixed-D columns and a mixed-D guard column in series, a 1260 diode array detector (DAD) and a 1260 refractive index detector (RID). The used eluent was DMA containing 50 mM of LiCl at a flow rate of 0.500 mL/min. The spectra were analyzed using the Agilent Chemstation software with the GPC add on. Molar mass and dispersity values were calculated against PMMA standards from PSS.

UV-Vis spectra were recorded on a Varian Cary 100 Bio UV-VIS spectrophotometer equipped with a Cary temperature and stir control. Samples were measured in quartz cuvettes with a pathlength of 1.0 cm in the wavelength range of 200-700 nm.

The fluorescence measurements were carried out on a Varian Cary Eclipse fluorescence spectrophotometer also equipped with a Cary temperature and stir control. The slit width of the excitation and emission were kept at 5 nm during the measurements.

Polymerization reaction mixtures were prepared in a VIGOR Sci-Lab SG 1200/750 Glovebox system, with less than 1 ppm of O_2 and H2O.

Polymerizations were conducted in a Biotage Initiator Microwave System with Robot Sixty with a temperature range of 40-250°C equipped with a variable magnetic stirrer (300-900 RPM) utilizing capped reaction vials. These vials were heated to 200 °C overnight and allowed to cool to room temperature under vacuum and filled with nitrogen prior to use. All microwave polymerizations were performed with temperature control (IR sensor).

Deionized water was prepared with a resistivity less than 18.2 MΩ x cm using an Arium 611 from Sartorius with the Sartopore 2 150 (0.45 + 0.2 µm poresize) cartridge filter.

Matrix assisted laser desorption/ionization time of flight mass spectroscopy (MALDI-TOF MS) was performed on an Applied Biosystems Voyager De STR MALDI-TOF mass spectrometer equipped with 2 m linear and 3 m reflector flight tubes, and a 355 nm Blue Lion Biotech Marathon solid state laser (3.5 ns pulse). All mass spectra were obtained with an accelerating potential of 20 kV in positive ion mode and in either reflectron or linear mode. The solutions were made in acetone and spotted on the plate in a trans-2- 3-(4-tert-butylphenyl)-2-methyl-2-propenylidene malononitrile (>98.0%, TCI) matrix.

The polymeric films were obtained by spin coating a polymer solution in $CHCl_3$ (10 mg/mL) on quartz plates using a SPIN150 device. The applied spin coating parameters included a spin speed of 2000 rpm, an acceleration of 500 rpm/sec and a spin time of 30s.

The thickness of the mono and dual fluorescent dye labelled PEtOx was measured using a stylus contact profilometer (Dektak 8).

The dual α, ω-fluorescent dye labeled PEtOx with a degree of polymerization (DP) 100 electrospinning solution was prepared by dissolving the polymer (14 wt%) and high molecular weight PEtOx (11 wt%) in a mixture of water/ethanol (30/70 vol/vol), resulting in a solution with 25 wt% total polymer concentration and was subsequently stirred at room temperature for 24 h. The electrospinning experiments were performed on a mono-nozzle setup with an 18-gauge needle, a tip-to-collector distance of 10 cm and a flow rate of 1 mL/h. The voltage was adapted in the range from 15 kV to 20 kV to enable a stable electrospinning process. The electrospinning process was performed in a climate chamber (Weisstechnik WEKK 10.50.1500) to maintain a relative humidity of 30% and a constant temperature of 25 °C.

Fiber morphology was examined using a scanning electron microscope (FEI Quanta 200 F or FEI Phenom desktop SEM) at an accelerating voltage of 20 kV. Sample preparation was done using a gold sputter coater (Balzers Union SKD 030 or Emitech K550X). The nanofiber diameters were measured using UTHSCSA ImageTool version 3.0, developed by the University of Texas Health Science Center. The average fiber diameters and their standard deviations are based on at least 15 measurements per sample.

^{1}H DOSY NMR spectra were measured and recorded on Bruker Avance III 400 MHz spectrometer at 25 °C. Samples were prepared at 1 mg mL^{-1} in deuterated solvents ($CDCl_3$, D_2O). Samples were stationary (not spinning) and the gradient strength was increased linearly from 2% to 95% over 64 steps. The maximum gradient strength used was 0.535 T/m. Bipolar rectangular gradients were used with a duration of 2.8 ms and the gradient recovery delay was 100 µs. Diffusion times were between 0.5 and 1.0 s. The spectrum was phased, and baseline corrected before 2D processing via Topspin 2.1.6 software (Bruker). The peak hydrodynamic radii (RHp) was calculated using the Stokes - Einstein equation.

$$D = \frac{k_B T}{(6\pi\eta R_H p)} \quad (1)$$

where sample viscosity (η) was determined via changes in the solvent diffusion compared to a blank solvent standard,[54] and the Boltzmann constant (KBe-1) concentration via serial dilution.

Cloud point temperatures (TCP) were measured on a Crystal16TM parallel crystallizer turbidimeter developed by Avantium Technologies connected to a recirculation chiller and dry compressed air. Aqueous polymer solutions (10 mg/mL) were heated from 20 to 95 ^{o}C with a heating rate of 0.5 ^{o}C /min followed by cooling to 2 ^{o}C at a cooling rate of 0.5 ^{o}C /min. This cycle was repeated three times. The TCPs are

reported as the 50% transmittance temperature in the second heating run.

Dynamic light scattering (DLS) was measured on a Zetasizer Nano-ZS Malvern apparatus (Malvern Instruments Ltd) using disposable cuvettes. The excitation light source was a He−Ne laser at 633 nm and the intensity of the scattered light was measured at an angle of 173°.This method measures the rate of the intensity fluctuation and the size of the particles is determined through the Stokes−Einstein equation. The concentration of the polymer solution was 1mg/mL in all cases.

Synthesis

Synthesis of single ω-fluorophore labeled poly(2-ethyl-2-oxazoline)s

All polymers were synthesized under similar conditions. The monomer concentration was 4 mol/L in Acetonitrile (ACN) for all polymerizations. The monomer/initiator [M]/[I] ratio was 10/1, 30/1, 50/1, 70/1 and 100/1, respectively. The solutions were prepared in a glove box under argon and the reactions were carried out in capped microwave vials. The polymerizations mixtures were heated to 140 °C under microwave irradiation for 71 s ([M]/ [I] = 10), 214 s ([M]/ [I] = 30), 307 s ([M]/ [I] = 50), 499 s ([M]/ [I] = 70), and 713 s ([M]/ [I] = 100) to reach almost full conversion. For the end-capping reactions, the vial was cooled down to room temperature and a solution of the corresponding acid in DMF 1.5-fold excess was added via a syringe through the septum of the capped microwave vial containing the living oligomers. Thereafter, TEA was added similarly in a two-fold molar excess relative to initiator. The given amounts were varied according to the used monomer to initiator ratios. The reaction solution was heated to 100 °C for 20 hours. After cooling to room temperature, the reaction mixture was diluted with chloroform and the solution was washed three times with saturated aqueous sodium hydrogen carbonate. Then the solution was washed with distilled water, brine, dried over MgSO4 and filtered. The solvent was evaporated under reduced pressure resulting a foamy polymer. The polymers were dissolved again in chloroform, precipitated in ice cold diethyl ether, and centrifuged for 10 minutes (7500 rpm) at 5 °C. The liquid was removed and the resulting precipitate was dissolved in DCM and evaporated under reduced pressure resulting in a white or yellow foam for the polymers modified with 1-pyrenebutyric acid or coumarin 343, respectively. Finally, the polymers were dried overnight in the vacuum oven at 50 °C. All homopolymers were obtained in high yields (> 80 %).

^{1}H NMR PEtOx-Py DP 30 (D30) (300 MHz, δ in ppm, $CDCl_3$): δ 8.30 – 7.68 (9H, Pyrene), 4.08 (s, 2H, CH_2-C=O-O), 3.38 (4H, N-CH_2-CH_2), 2.95 (2H, O-O=C-CH_2), 2.89 (2H, CH_3-N-CH_2), 2.26 (2H, CH_3-CH_2-C=O and CH_2-CH_2-Py), 1.05 (3H, CH_3-CH_2-C=O).

Kinetic investigation of the microwave-assisted homopolymerization of EtOx initiated with 1-(bromomethyl)pyrene

A stock solution consisting of monomer, initiator (1-(bromomethyl)pyrene) and solvent (acetonitrile), was prepared in the glovebox. The initial monomer concentration was 4 mol/L for all the experiments. After stirring for 10 minutes the stock solution was divided in separate 0.5-2.0 mL Biotage reaction vials in portions of 800 µL with automated pipettes. After preparing the polymerization mixtures, they were placed in the autosampler of the Biotage microwave and were left to react at 140°C for varying times. The points of the kinetic studies are all based on individual polymerization reactions. The sample of 1 second was always included to determine the influence of the heating ramp. After the polymerizations, the polymerization mixture was diluted with 1 mL chloroform and stirred for 10 minutes. Two samples of 100 µL were taken. The first 100 µL sample was taken for GC analysis and was further diluted with chloroform until a total volume of 1.5 mL. The second 100 µL was taken for SEC analysis and was further diluted with DMA until 1.5 mL. The samples were filtered over syringe filters with membranes made of hydrophilic polytetrafluoroethylene (PTFE) with a pore size of 0.22 µm. SEC analysis was performed to determine the number average molar mass (Mn) and dispersities (Đ).

Synthesis of single α-pyrene labeled poly(2-ethyl-2-oxazoline)s (iD)

All polymers were synthesized under similar conditions. The monomer concentration was 4 mol/L in ACN for all polymerizations. The monomer (1-(bromomethyl)pyrene))/ initiator [M]/[I] ratio was 10/1, 30/1, 50/1, 70/1 and 100/1, respectively. The solutions were prepared in a glove box under argon and the reactions were carried out in capped microwave vials. The polymerizations mixtures were heated to 140°C under microwave irradiation 183 s ([M]/ [I] = 10), 548 s ([M]/ [I] = 30), 913 s ([M]/ [I] = 50), 1279 s ([M]/ [I] = 70), and 1827 s ([M]/ [I] = 100) to reach almost full conversion. The polymerizations were quenched by the addition of a 1 M KOH solution in MeOH. The polymers were precipitated in ice cold diethyl ether and centrifuged for 10 minutes (7500 rpm) at 5°C. The liquid was removed, and the resulting precipitate was dissolved in DCM and reprecipited in diethyl ether. Then the polymers were redissolved in DCM and evaporated under reduced pressure resulting in a white foam. Finally, the polymers were dried overnight in the vacuum oven at 50°C. All α-pyrene labeled homopolymers were obtained with good purities and in high yields.

Synthesis of dual-labeled poly(2-ethyl-2-oxazoline)s (DA)

All polymers were synthesized using the same procedure presented above for α-pyrene labeled poly (2-ethyl-2-oxazoline)s. For the end-capping reactions, the vial was cooled down to room temperature and a solution of the Coumarin 343 in DMF 1.5-fold excess was added via a syringe through the septum of the capped microwave vial containing the living oligomers. Thereafter TEA was added similarly in a two-fold molar excess relative to initiator. The given amounts were varied according to the used monomer to initiator ratios. The reaction solution was heated to 100°C for 20 hours. After cooling to room temperature, the reaction mixture was diluted with chloroform and the solution was washed three times with saturated aqueous sodium hydrogen carbonate. Then the

solution was washed with distilled water, brine, dried over magnesium sulphate and filtered. The solvent was evaporated under reduced pressure resulting a foamy polymer. The polymers were dissolved again in chloroform, precipitated in ice cold diethyl ether, and centrifuged for 10 minutes (7500 rpm) at 5°C. The liquid was removed and the resulting precipitate was dissolved in DCM and evaporated under reduced pressure resulting in yellow foam. Finally, the polymers were dried overnight in the vacuum oven at 50°C. All dual labeled homopolymers were obtained with good purities and in high yields.

^{1}H NMR Py-PEtOx-Cou343 DP 30 (DA30) (300 MHz, $CDCl_3$) δ 8.36 – 7.87 (9H, Pyrene), 6.86 (1H, *CH*-C), 5.27 (2H, pyrene-*CH_2*), 4.33 (2H, CH_2-*CH_2*-O), 3.29 (4H, NH-*CH_2*-*CH_2*), 2.75 (4H, N-*CH_2*-*CH_2*), 2.26 (4H, C-O=C-*CH_2*-CH_3 and C-*CH_2*-CH_2), 1.15 – 0.88 (3H, CH_2-CH_3).

Synthesis of high molecular weight non-functionalized PEtOx

The high molecular weight non-functionalized PEtOx was synthesized at lower temperatures and a lower monomer conversion (75%) was targeted to reduce chain transfer reactions. The polymerization solution was prepared in a glovebox in a pre-dried and silanized 1 L schlenck flask. In short, 161.5 mL of EtOx (1333 equivalents, 1.6 mol) and 181 µL of MeOTs (1 equivalent, 1.2 mmol) were added to 238 mL of chlorobenzene to obtain a 4 M monomer solution. The solution was subsequently heated to 80°C for 29 hours, until a monomer conversion of 75% was reached, which was determined by GC. The polymerization was terminated by the addition of 3 mL of a 1 M KOH solution in MeOH (2.5 molar equivalents relative to initiator), and the resulting solution was stirred overnight at room temperature. Next, distilled water was added 550 mL of milliQ water was added and the mixture was evaporated under reduced pressure, this procedure was repeated 5 times to remove chlorobenzene. The aqueous polymer solution was subsequently dialyzed (molecular weight cut-off 3.5 kDa) and freezedried to obtain the pure polymer.

^{1}H NMR PEtOx (400 MHz, $CDCl_3$) δ 3.61 – 3.05 (4H, N-*CH_2*-*CH_2*), 2.45 – 2.11 (2H, CH_3-*CH_2*-C=O), 1.22 – 0.87 (3H, *CH_3*-CH_2-C=O) SEC: Mn = 69 kDa, Mp = 85 kDa, Đ = 1.39.

FRET Calculations

The Förster theory shows that FRET efficiency (EFRET) varies as the sixth power of the distance between two molecules (equation 1). To calculate the FRET efficiency, one has to determine the spectral overlap integral J and the interchromophoric distance r.

$$E_{FRET} = \frac{1}{1+\left(\frac{r}{R_0}\right)^6} \quad (2)$$

Where R_0 is the distance between the two molecules at 50% FRET efficiency and r being the interchromophoric distance for the experiment. R_0 can be calculated using equation 2.

$$R_0 = 0.02108\ (\kappa^2\ \phi_D\ n^{-4}\ J)^{\frac{1}{6}} \quad (3)$$

Where ϕ_D is the fluorescence quantum yield of the donor in the absence of the acceptor, κ^2 is the orientation factor of transition dipole moment between donor and acceptor; κ^2 can take values between 0 and 4. In the present case we have considered κ^2= 2/3 (when both dyes are freely rotating and can be considered to isotropically oriented during the excited state lifetime), n is the refractive index of the medium, and J is the spectral overlap integral calculated as:

$$J = \int \varepsilon_{Acceptor}(\lambda)\lambda^4\overline{I_D}(\lambda)\, d\lambda \quad (4)$$

Where $\varepsilon_{Acceptor}(\lambda)$ is the acceptor molar extinction coefficient at the wavelength is λ, λ is the wavelength and $\overline{I_D}(\lambda)$ is the normalized emission spectrum of the donor. By integrating this over the entire spectrum one can calculate the *J* value, the unit of $J(\lambda)$ is M^{-1} cm^{-1} nm^4. The quantum yield of the pyrene labeled polymers was determined as described in the next section.

The efficiency of FRET can be determined by steady-state measurements and is expressed as equation (4). From this r can be calculated as follows:

$$E_{FRET} = 1 - \frac{F_{DA}}{F_D} \quad (5)$$

Where F_{DA} and F_D are the donor fluorescence intensities with and without an acceptor respectively. The FRET efficiency was determined by donor quenching method.

The actual distance r between donor and acceptor is given by:

$$r = R_0 \cdot \left(\frac{1}{E_{FRET}} - 1\right)^{1/6} \quad (6)$$

The quantum yield of the labeled polymers was determined via comparison with anthracene in ethanol which has a known quantum yield of 0.27.[59] The quantum yield (Φ_X) was calculated using equation 7:

$$\Phi_X = \Phi_{ST}\left(\frac{\mathrm{Grad_X}}{\mathrm{Grad_{ST}}}\right)\left(\frac{n_X^2}{n_{ST}^2}\right) \quad (7)$$

where X represents the analyte, ST the standard (anthracene/ethanol), Grad the gradient of integrated fluorescence emission / absorbance and n the refractive index of solvents.

Results and discussion

Polymer Synthesis and Characterization

A series of well-defined PEtOx polymers having a single donor or acceptor at the ω-chain end with varying degree of polymerization were synthesized by CROP of EtOx initiated with methyl tosylate (MeOTs) followed by termination with either 1-pyrenebutyric acid (Py) or coumarin 343 (Cou 343) (Figure 1a). The obtained polymers showed narrow molar mass distributions (Đ ≤ 1.15) as well as high degree of functionalization (> 92%) as determined by ^{1}H-NMR spectroscopy (Table 1 and Figure S1-S4). Furthermore, the number average molecular weight (Mn) increased with increasing target degree of polymerization (DP). MALDI-TOF-MS analysis revealed a single polymer distribution in all cases and the exact masses of the

corresponding peaks fit to a PEtOx structure with both methyl, and pyrene or coumarin end-groups (Figure S5-S6). Taking advantage of the synthetic versatility of PAOx, α,ω-dual-functionalized PEtOx could be easily obtained by using 1-(bromomethyl)pyrene as initiator instead of MeOTs in combination with termination with Cou 343 (Figure 1a). To investigate the suitability of 1-(bromomethyl)pyrene as initiator for the CROP of EtOx, we performed a kinetic study with a polymerization temperature of 140 °C and a monomer concentration of 4M in acetonitrile. The first-order kinetic plot of monomer consumption with respect to the reaction time revealed a linear relationship (Figure 1b), thus demonstrating a constant amount of propagating species indicative of the absence of termination reactions. Moreover, Mn increased linearly with conversion, while the dispersity remained below 1.15, indicating the absence of significant chain transfer side reactions (Figure 1c and Table 1). As such, it can be concluded that 1-(bromomethyl)pyrene is a good initiator for the CROP of EtOx resulting in a living polymerization.

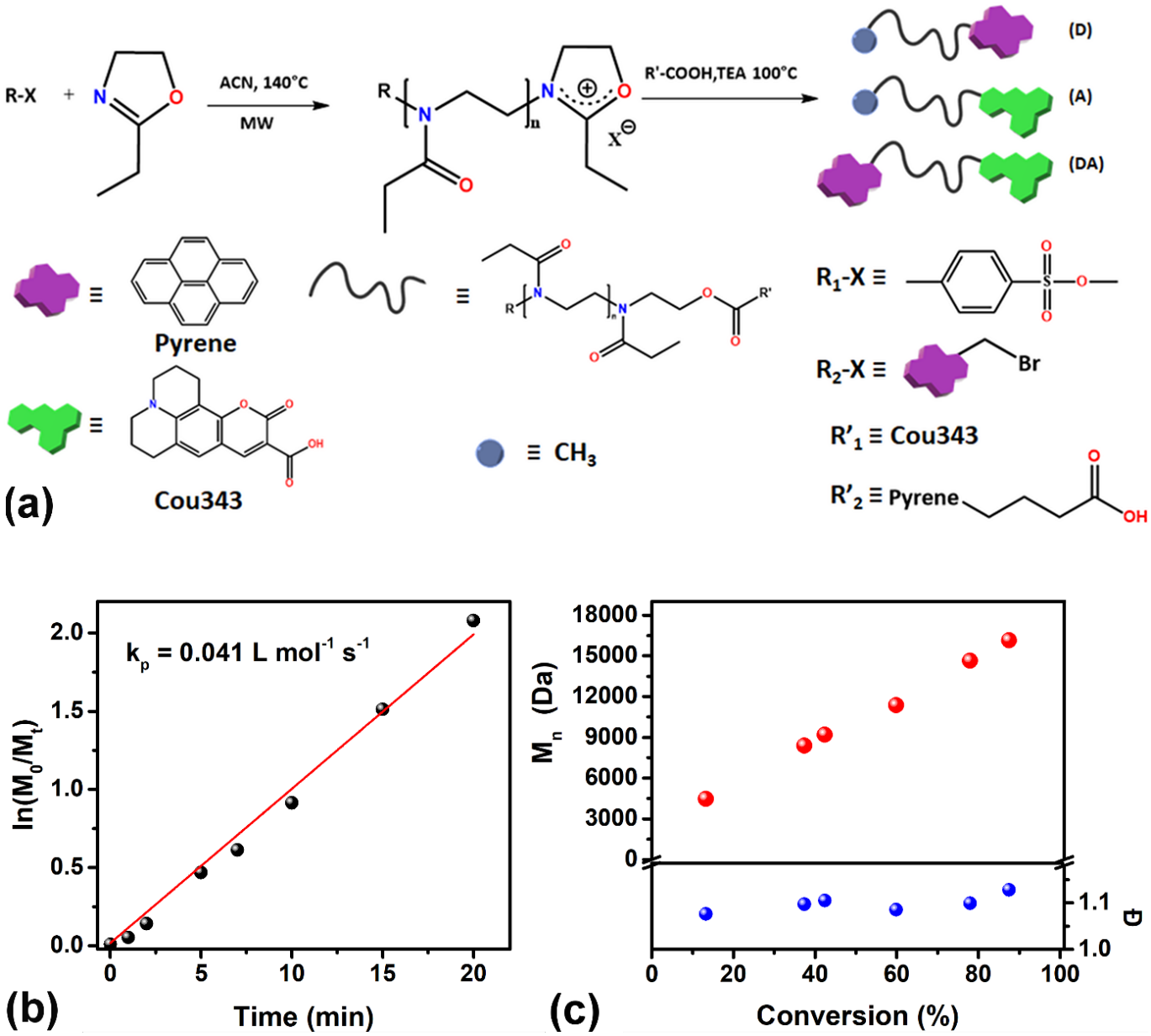

Figure 1. Schematic representation of the reaction path to obtain single as well as dual donor and/or acceptor labeled PEtOx polymers; (b) first-order kinetic plot, and (c) corresponding number-average molecular weight (Mn) against conversion plot, including dispersities (Đ) for the CROP of EtOx initiated with 1-(bromomethyl) pyrene at 140 °C in acetonitrile with 4 M monomer concentration for a targeted DP of 100. Mn values were determined by SEC analysis, calculated against poly(methylmethacrylate) (PMMA) standards.

The polymerization rate constant was calculated form the linear fit of the first order kinetic plot, assuming that the concentration of propagating species is equal to the initial initiator concentration, i.e., complete initiation. The value obtained is similar as the kp that has been reported for CROP of EtOx initiated with benzyl bromide under similar conditions.[60] This method was subsequently applied for the

preparation of the dual-functionalized PEtOx having both pyrene and Cou 343 end-groups.

Table 1. Structural characterization of the synthesized single and dual fluorescent dye-labeled PEtOx.

Polymer code	Yield (%)	DP[a]	f (%)[b]	M_n (kg/mol)[c]	M_n (kg/mol)[d]	Đ[c]	T_{CP} (°C)[e]
D10	80	10	93	2.0	1.2	1.02	n.s.
D30	97	30	94	5.9	2.9	1.09	61.9
D50	80	50	95	10.9	5.1	1.09	64.2
D70	80	70	94	12.6	6.9	1.09	65.3
D100	87	100	93	23.3	10.1	1.15	62.5
A10	84	10	95	1.9	1.1	1.19	n.s.
A30	81	30	96	5.9	3.0	1.08	79.0
A50	94	50	93	10.2	5.1	1.08	76.2
A70	96	70	96	13.1	6.8	1.10	71.9
A100	87	100	92	19.7	9.9	1.15	69.9
DA10	85	10	94	2.1	1.1	1.18	n.s.
DA30	85	30	92	6.0	3.1	1.09	13.9
DA50	88	50	91	9.5	4.9	1.09	27.3
DA70	83	70	93	13.6	7.0	1.12	34.9
DA100	85	100	94	20.4	10.0	1.15	41.7

[a]Theoretical degree of polymerization.

[b]Degree of functionality calculated from the aromatic signals of the dye and the methyl signal of the polymer side chain as calculated from the ^{1}H NMR spectra.

[c]Determined from DMA SEC using PMMA calibration.

[d]Determined from MALDI-TOF-MS.

[e]Cloud point temperature in deionized water (10 mg/mL; 0.5°C/min).

The degree of functionalization was found to be over 90 % by 1H NMR spectroscopy, which is comparable with the one obtained for single-labeled polymers obtained by termination (Table 1 and Figure S7). MALDI-TOF-MS and SEC- RI/UV analysis further proved the successful incorporation of both dyes (Figures S8 and S9). α-Pyrene functionalized polymers (Py PEtOx; iD10-100) were also synthesized with 1-(bromomethyl)pyrene as initiator as control samples and used for evaluating the FRET efficiency in the dual labeled PEtOx. The polymers showed the expected molecular weight and low dispersities indicating their defined nature (Table S1 and Figure S10).

FRET Analysis in Solution

After the successful preparation of the dye-functionalized PEtOx, we focused our attention on their fluorescence behavior in solution to evaluate the FRET. The intermolecular FRET transfer between complementary ω-dye-labeled polymer chains was investigated in chloroform. The fluorescence emission spectra of the individual donor or acceptor labeled polymers (D10-100, A10-100) displayed the same fluorescence as the corresponding organic fluorophores as expected, since the ester linkage to the polymer chain has a minimal influence on the conjugated system of the dyes (Figure S11). Unexpectedly, the emission spectra of the pyrene-initiated iD10-100 polymers were quite different from the pyrene-terminated D10-100 polymers (Figure S14). At the same fluorophore concentration, the fluorescence intensity of the Py initiated PEtOx was lower, while the ratio between I1/I5 decreased, thus suggesting a more hydrophilic microenvironment in the case of ω-Py labeled polymer. Such a behavior indicates a lower exposure of ω-Py units to the solvent compared to α-Py labeled PEtOx due to a higher shielding effect of the polymeric chains, also promoted by the propyl flexible spacer. This is a surprising observation as the chemical structures of these labels are distinct only by the covalent linker to the polymer backbone (ester linkage compared to methyl separator), however, the influence of the conjugation on the emissive properties can not be completely ruled out.

Next, the dye-terminated polymers were mixed in a 1:1 molar ratio between the fluorophores at 10 μM concentration, and

after selective excitation of the donor at 345 nm, the emission spectrum showed donor as well as acceptor emission, thus suggesting the occurrence of intermolecular energy transfer (Figure 2). The FRET efficiency was rather low around 10 %, independent of the DP of the PEtOx chains (Figure 2, S12 and S13 a), which is similar to the FRET efficiency between the two fluorophores (i.e., 9.6 % FRET efficiency) at 10 µM (Figure S11 and S13b). These results indicate that at this low concentration of 10 µM the fluorophores are too far apart for efficient FRET. Consequently, connecting the two fluorophores together through a polymeric spacer should increase the FRET efficiency, by bringing them into closer proximity. Next, the fluorescence of α-Py labeled PEtOx was investigated.

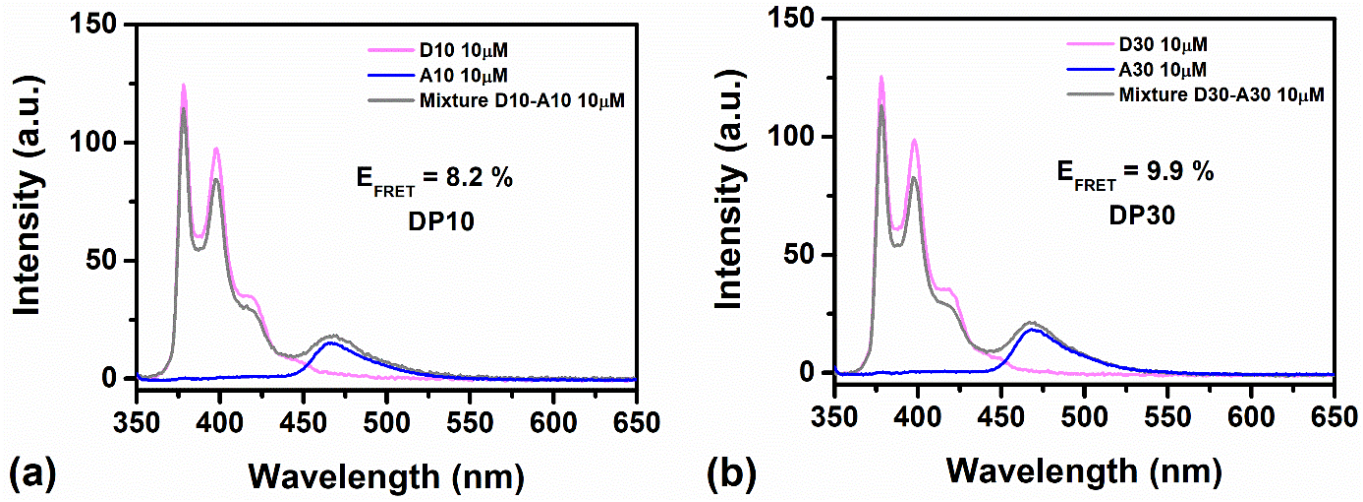

Figure 2. Emission spectra of: (a) D10, A10 and equimolar mixture of D10 and A10 in $CHCl_3$, and (b) D30, A30 and equimolar mixture of D30 and A30 in $CHCl_3$. In all cases, the excitation wavelength was 345 nm, and the concentration of the pyrene fluorophore was 10µM.

Fluorescence spectroscopy of the donor-acceptor labeled polymers (DA10-100) demonstrated a significant increase in the emission of the acceptor, upon excitation of the donor (Figure 3). This enhanced emission can be assigned to the intramolecular FRET taking place between the fluorophores, as we already demonstrated that intermolecular FRET efficiency is very low at the used 10 µM concentration. The FRET efficiency increases from 15.1% to 79.2% with decreasing the degree of polymerization from 100 to 10, because of the smaller distance between the two fluorophores (Table 2). The energy transfer is affected not only by the chain length of the polymer but also by the solvent and the temperature. Consequently, we expanded our studies to aqueous medium because PEtOx is a biocompatible water-soluble polymer, which also displays thermoresponsive behavior in water. Moreover, FRET could represent an efficient and simple tool to determine the influence of the solvent on the conformational changes of PEtOx. An 8-fold increase in the emission intensity of the α-single pyrene labeled PEtOx was observed when switching from $CHCl_3$ to water, while only a small variation was observed for Cou343 labeled PEtOx (Figure S15). This behavior can be explained by the higher quantum yield of Py-PEtOx in water as compared to $CHCl_3$ (Table S1) due to solvent pyrene-interactions as well as the change in conformation of the polymer chains, which restricts the collisional quenching of the fluorophore. The data is in accordance with the results previously reported by Winnik et al. demonstrating that going from an apolar to a polar solvent enhances the molar extinction coefficient of the O-O band of pyrene (Figure S15).[61] For A50 we noticed a 25 nm bathochromic shift when switching from $CHCl_3$ to water. Moreover, the emission band at 583 nm showed a hypochromic shift (i.e., fluorescence quenching), which can be ascribed to the reduced solubility of the polymer in water and hydrogen bonding interactions.[62] The FRET efficiency is greatly enhanced in water compared to $CHCl_3$, suggesting a decreased distance between the fluorophores. The increased FRET can be ascribed to the decrease in solvent quality for the highly hydrophobic fluorophores, possibly leading to the formation of hydrophobic domains, which maximizes the FRET transfer. The FRET dependency on chain length follows the same, expected trend as in $CHCl_3$, that a lower FRET efficiency is observed at higher DP. The lower intensity of the emission of Cou343 registered for DA10 could be explained by the reduced solubility of this polymer in water and the high tendency for aggregation, which leads to fluorescence quenching.

Figure 4 shows the distance dependence of FRET efficiency for the donor-acceptor dual-labeled PEtOx, as calculated from the FRET efficiency obtained from fluorescence spectroscopy. The 50% transfer efficiency corresponds to a value of Förster radius (R_0) of 4.5 nm in $CHCl_3$ and 4.6 nm in water, respectively. Because chloroform is a better solvent for the dye-labeled polymers, the PEtOx chains adopt a more extended conformation leading to a larger average donor-acceptor distance than in water (Table 2).

Table 2. Energy transfer parameters for dual dye labeled PEtOx in $CHCl_3$, H_2O, and in a film.

Polymer code	DP	Solvent	R_0 (nm)[a]	$J \cdot 10^{15}$ ($M^{-1} \cdot cm^{-1} \cdot nm^4$)[b]	E_{FRET} (%)[c]	r (nm)[d]	R_H (nm)[e]
DA10	10	$CHCl_3$	4.5	12.9	79.2	3.6	4.97
DA30	30	$CHCl_3$	4.5	12.0	40.2	4.8	5.45
DA50	50	$CHCl_3$	4.5	12.0	32.1	5.1	6.55
DA70	70	$CHCl_3$	4.5	12.0	16.0	5.9	6.26
DA100	100	$CHCl_3$	4.5	12.3	15.1	6.0	6.72
DA10	10	H_2O	4.6	6.9	96.4	2.5	10.89
DA30	30	H_2O	4.6	9.8	92.7	3.0	13.62
DA50	50	H_2O	4.6	9.9	83.6	3.5	17.75
DA70	70	H_2O	4.6	9.8	72.5	3.9	21.89
DA100	100	H_2O	4.6	9.5	52.6	4.5	27.94
DA10	10	Film	5.3	38.8	99.9	1.7	-
DA30	30	Film	5.3	47.9	99.9	1.7	-
DA50	50	Film	5.3	40.0	99.8	1.9	-
DA70	70	Film	5.3	39.4	99.6	2.1	-
DA100	100	Film	5.3	37.1	99.5	2.2	-

[a]Förster radius calculated using equation 3.

[b]Spectral overlap integral calculated using equation 4.

[c]Energy transfer efficiency calculated using equation 5.

[d]Donor-acceptor distance calculated using equation 6.

[e]Hydrodynamic radius determined from DOSY NMR measurements using equation 1.

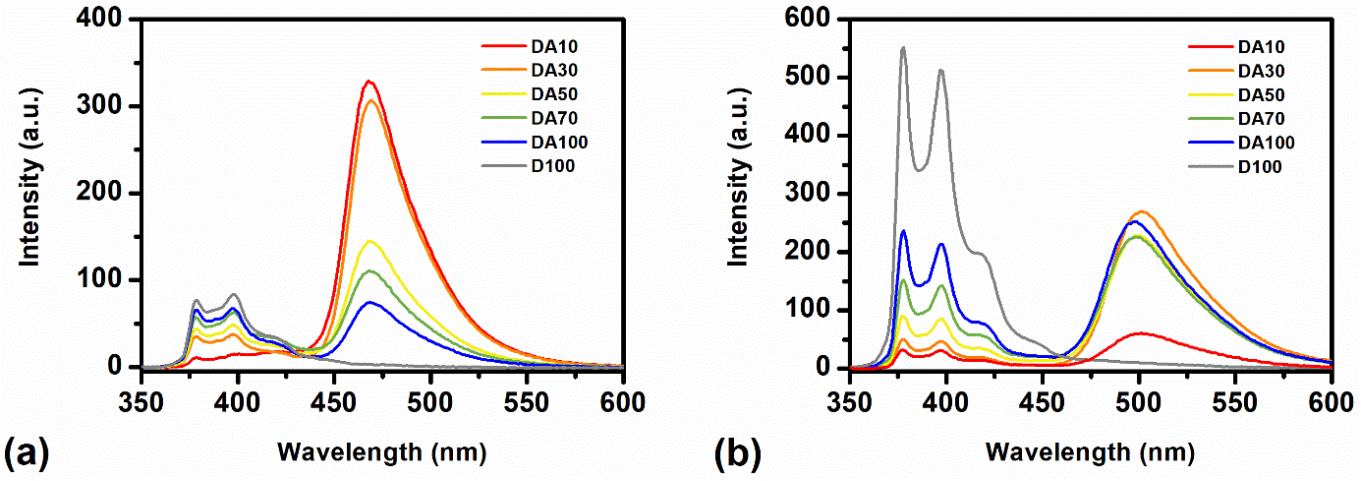

Figure 3. Emission spectra of: (a) DA10-DA100 in CHCl3, and (b) DA10-DA100 in H2O. In all cases, the excitation wavelength was 345 nm, and the concentration of the pyrene was 10μM.

Figure 4 shows the distance dependence of FRET efficiency for the donor-acceptor dual-labeled PEtOx, as calculated from the FRET efficiency obtained from fluorescence spectroscopy. The 50% transfer efficiency corresponds to a value of Förster radius (R_0) of 4.5 nm in $CHCl_3$ and 4.6 nm in water, respectively. Because chloroform is a better solvent for the dye-labeled polymers, the PEtOx chains adopt a more extended conformation leading to a larger average donor-acceptor distance than in water (Table 2). If the chain end-to-end distance (r) is equated to the polymer R_G, then information about the shape and compactness of the polymer can be determined if the hydrodynamic radius (R_H) is also known.32 Consequently, DOSY-NMR measurements were performed (Figure S18) to determine the R_H of the dual labeled polymers and the results are listed in Table 2. In $CHCl_3$ the R_H increase from 5 nm to 6.7 nm as the DP increases from 10 to 100, which is roughly in line with the chain end-to-end distance r. Comparatively in an aqueous environment the chain end-to-end distance increases from 2.5 nm and 4.5 nm while the diffusion measurements predict the polymers to have an RH ranging from 13 nm to 28 nm. Additional hydrodynamic radii of singly labeled polymers are shown in Table S2. The ratio of ρ (R_G / R_H) in $CHCl_3$ increases from 0.7 to 0.9, whereby theoretically a ρ of 0.778 corresponds to homogeneous hard sphere dissolved polymers while a ρ of 0.87 to 0.98 indicates oblate ellipsoid structures. These data suggest that the dual-labeled PEtOx are well solvated in chloroform whilst this does not appear to be the case in the aqueous systems. Due to the increased RH seen in the aqueous systems this would suggest a ρ of < 0.3, which is not feasible. These higher R_H values in water suggest that the dye labeled polymers either form minor aggregates, chain-to-chain intramolecular interactions artificially increase the hydrodynamic radii or the polymer chain ends are interacting and the polymer is no longer obeying the freely jointed chain model. To investigate this observation, additional dynamic light scattering (DLS) measurements were carried out (Figure S19) providing further evidence that in aqueous solution there is agglomeration of multiple polymer chains.

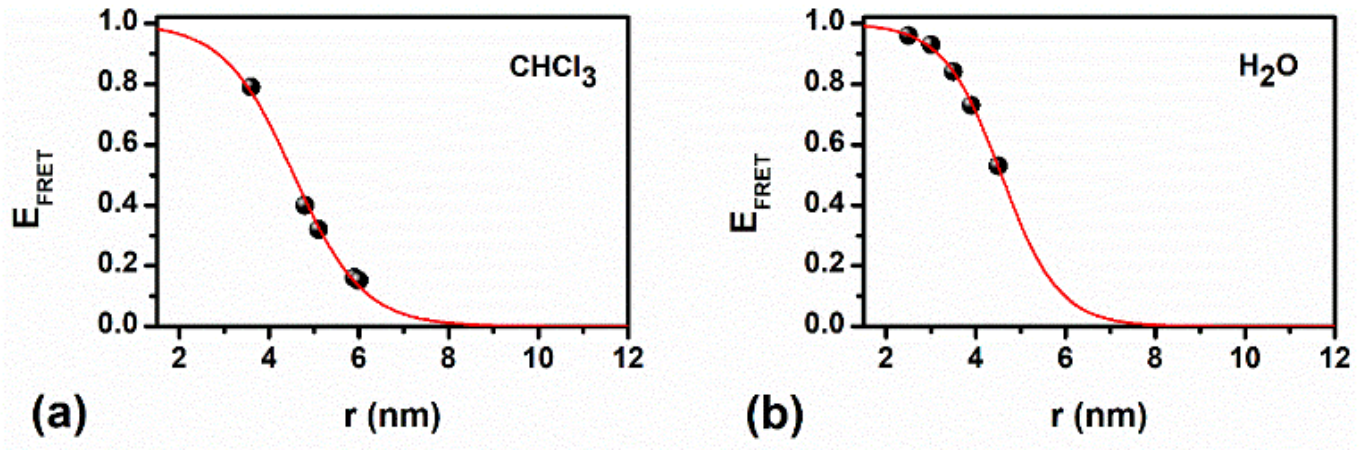

Figure 4. Distance dependence of FRET efficiency in α, -ω-dye labeled PEtOx polymers in: (a) CHCl3, and (b) H2O showing the characteristic sigmoidal curve.

Thermoresponsive FRET Behavior

As PEtOx is thermoresponsive in aqueous solution, we studied the thermoresponsive behavior of the dual dye-labeled polymers to evaluate their use for potential sensing applications. Cloud point temperatures (T_{CP}) and turbidimetry profiles of the PEtOx dye labeled polymers are provided in Table 1 and Figures S20-21. The presence of the hydrophobic dye end-groups reduced the polymer solubility in water, and most of the dye-labeled PEtOx displayed LCST behavior. The results are in accordance with the previous report of Jordan et al. showing that incorporation of hydrophobic end-groups decreases the T_{CP}.[63] As expected, the polymer solubility and, thus, the T_{CP} increased with increasing chain length, whereby A10, D10, and DA10 were not completely water soluble at the investigated concentration of 10 mg·mL^{-1}. The Py-functionalized PEtOx showed a lower T_{CP} than the Cou343-functionalized PEtOx, which can be explained by the difference in the hydrophobicity of the two fluorophores. The dual-labeled polymers showed even lower T_{CP}s, due to the higher overall hydrophobicity. Lower T_{CP}s were registered for iD30-100 values as compared to their counterparts D30-100 polymers (Figure S20) evidencing once more the importance of Py positioning on the polymeric chain.

The thermo-sensing ability of the fluorophore labeled PEtOx polymers was investigated by temperature controlled fluorescence spectroscopy at a polymer concentration of 1 mg·mL^{-1}. Single labeled Py polymers showed a marked decrease in the fluorescence intensity with increasing temperature (Figure S22a). In contrast, the fluorescence intensity of single labeled Cou343 PEtOx slightly increased with increasing temperature (Figure S22b). The analysis of the fluorescence spectra of the DA polymers reveals a decrease of the Cou343 FRET emission and a 5 nm hypsochromic shift with increasing temperature (Figure 5 and Figure S23). The blue shift of the emission could be correlated with a change in the polarity of the local environment and disruption of hydrogen bonding between Cou343 and the solvent due to collapse of the polymeric chains. The temperature-dependent emission that was observed for the DA PEtOx can be attributed to a decrease of FRET efficiency due to the lower fluorescence quantum yield of the pyrene with increasing temperature. Moreover, the threshold of the emission decrease is dependent on the chain length of the polymer, increasing from 40 to 60 °C. These threshold values nicely correspond with the T_{CP} of the DA30-100 polymers (Figure 5, Figure S23 and S24), thus demonstrating the applicability of the dual labeled PEtOx polymers as fluorescent probes for temperature sensing.

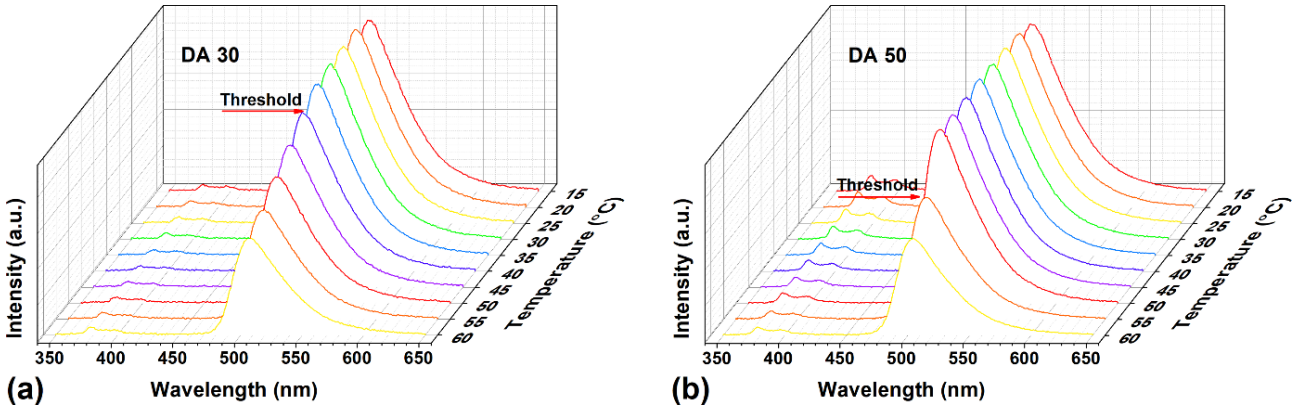

Figure 5. Fluorescence spectra as a function of temperature for (a) DA30, and (b) DA50, respectively. In all cases, the excitation wavelength was 345 nm, and the concentration of the polymer was 1 mg·mL^{-1}

FRET Analysis in Solid State

The energy transfer process of the dual labeled PEtOx polymers was also studied in the solid state (e.g., films and nanofibers) in order to investigate their potential to be used in practical applications. Thin films were obtained by spin-coating of the DA 10-100 polymers as well as the single labeled PEtOx-Py D10-100. The emission intensity (I_D) of the D10-100 was used to calculate the FRET efficiency.[16] A value of 0.476 was used for the orientation factor, which corresponds to dipoles

randomly oriented in a rigid medium.[64, 65] The R_0 distance in the film was determined to be 4.7 nm, while the calculated FRET efficiency was higher than 99%, regardless the DP of the polymer. In the film, the two fluorophores were found to be in close proximity (i.e., r ≈ 1.4 nm), thus increasing the possibility of energy transfer.

Next, we investigated the use of DA100 for electrospun nanofibers due to its potential applications in photonics area as laser and/or optical sensor. Nanofibers were prepared by electrospinning of a polymer solution consisting of a mixture of DA100 (14 wt%) and a high molecular weight non-functionalized PEtOx (11 wt%; Mn: 70kDa; Mp: 85kDa; Đ: 1.39), which was added to aid to electrospinnability of the solution by enhancing its viscosity.[66] The SEM analysis of the obtained nanofibers revealed the formation of homogeneous, smooth, uniform and beadless fibers with a diameter of 405 ± 84 nm. D100 nanofibers were also prepared as reference material. Fluorescence analysis revealed the FRET in the electrospun DA100 nanofibers (Figure 6). Irradiation with 345 nm light led to Cou343 emission at 500 nm, while the emission of Py was strongly diminished. The inset in Figure 6 also nicely illustrates the change in color of the nanofibers upon 345 nm light irradiation. These preliminary measurements unveil the possibility to further develop these materials for future applications in areas such as the detection of explosives, heavy metal ions, solar cells and/or bioimaging.

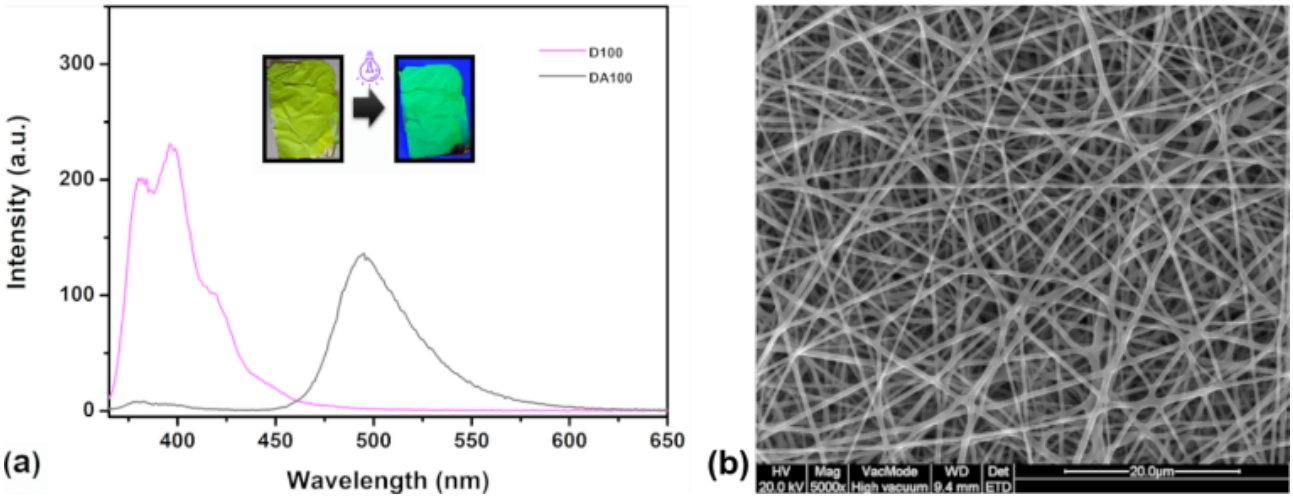

Figure 6. (a) Emission spectra of D100 and DA100 nanofibers, the inset shows the change in color upon irradiation with 345 nm light; (b) SEM image of the DA 100 nanofibers.

Conclusions

In summary, this work demonstrated the synthesis of α- or ω-single and α,ω-dual fluorophore labeled PEtOx polymers with high yields, low dispersity, and a high degree of functionalization. As expected, the intermolecular FRET transfer between ω-labeled polymers was low and comparable with the energy transfer between the organic fluorophores. However, connecting the two fluorophores via a PEtOx chain resulted in high intramolecular FRET efficiency, which was more efficient for shorter polymers. Improved FRET efficiency was also demonstrated for the α,ω-dual fluorophore labeled PEtOx in aqueous media as compared to $CHCl_3$ as organic solvent. The use of these polymers as fluorescent probes for temperature sensing was demonstrated based on the change in FRET efficiency with increasing temperature. The PEtOx optical thermometers showed a temperature sensing regime from 40 to 60 °C. Moreover, films and nanofibers were successfully obtained using these materials, while maintaining their emissive properties in the solid state, without altering the energy transfer efficiency. Our results provide in-depth understanding of the chain length and solvent effect on the FRET efficiency and demonstrated the importance of locating the chromophores on the same polymer. It is expected that these polymer structures could be used for investigating many photophysical phenomena, as well as the polymer chain conformation. Moreover, the near-quantitative labeling strategy expands the methodology for the preparation of poly(2-oxazoline)s with functional groups located at specific sites. Furthermore, these polymers could find useful applications in solar cells as well as in fluorescence microscopy, which is under current investigations in our lab.

Conflicts of interest

There are no conflicts to declare.

Supporting Information

Supporting results for synthesis of the dye functionalized PEtOx. Fluorescent properties, DOSY, and thermoresponsive behavior of the fluorescent dye labeled PEtOx polymers.

Acknowledgements

Results in this paper were obtained within the framework of the FWO Strategic Basic Research grant 1SA4719N of Ronald Merckx.

Furthermore, Richard Hoogenboom would like to thank continued support from Ghent University and FWO. Dr Thomas Swift would like to thank the Royal Society of Chemistry for travel grant funding to visit Prof Hoogenboom's laboratory (RM1602-1695).

Notes and references

The authors declare the following competing financial interest(s): Richard Hoogenboom is one of the founders of Avroxa BVBA that commercializes poly(2-oxazoline)s as Ultroxa. The other authors declare no competing financial interest.

1 Z. Sekkat and W. Knoll, in Molecular Switches, eds. B. L. Feringa and W. R. Browne, WILEY-VCH Verlag & Co. KGaA, Weinheim, Germany, 2011, DOI: 10.1002/9783527634408.ch13, pp. 423-515.
2 W. Knoll, in Mater. Sci. Technol., eds. R. W. Cahn, P. Haasen and E. J. Kramer, Weinheim Wiley-VCH, 2006, DOI: 10.1002/9783527603978.mst0143.
3 J. Chen, W. Zhong, Y. Tang, Z. Wu, Y. Li, P. Yi and J. Jiang, Macromolecules, 2015, 48, 3500-3508.
4 J. A. Delaire and K. Nakatani, Chem. Rev., 2000, 100, 1817-1846.
5 S. Kundu and A. Patra, Chem. Rev., 2017, 117, 712-757.
6 M. P. Robin and R. K. O'Reilly, Polym. Int., 2015, 64, 174-182.
7 F. A. Nicolescu, V. V. Jerca, I. C. Stancu, D. S. Vasilescu and D. M. Vuluga, Des. Monomers Polym., 2010, 13, 437-444.
8 S. Ulrich, J. R. Hemmer, Z. A. Page, N. D. Dolinski, O. Rifaie-Graham, N. Bruns, C. J. Hawker, L. F. Boesel and J. Read de Alaniz, ACS Macro Lett., 2017, 6, 738-742.
9 P. Weis, D. Wang and S. Wu, Macromolecules, 2016, 49, 6368-6373.
10 P. Weis and S. Wu, Macromol. Rapid Commun., 2018, 39, 1700220.
11 A. F. Nicolescu, V. V. Jerca, A.-M. Albu, D. M. Vuluga and C. Draghici, Mol. Cryst. Liq. Cryst., 2008, 486, 38/[1080]-1049/[1091].
12 M. Beija, M.-T. Charreyre and J. M. G. Martinho, Prog. Polym. Sci., 2011, 36, 568-602.
13 M. Chen, K. P. Ghiggino, A. W. H. Mau, E. Rizzardo, S. H. Thang and G. J. Wilson, Chem. Commun., 2002, 2276-2277.
14 M. Chen, K. P. Ghiggino, S. H. Thang and G. J. Wilson, Angew. Chem. Int. Ed., 2005, 44, 4368-4372.
15 P. J. Roth, M. Haase, T. Basché, P. Theato and R. Zentel, Macromolecules, 2010, 43, 895-902.
16 Y. Sha, D. Qi, S. Luo, X. Sun, X. Wang, G. Xue and D. Zhou, Macromol. Rapid Commun., 2017, 38, 1600568.
17 J.-S. Huang, T. Goh, X. Li, M. Y. Sfeir, E. A. Bielinski, S. Tomasulo, M. L. Lee, N. Hazari and A. D. Taylor, Nat. Photonics, 2013, 7, 479.
18 H. Sahoo, J. Photochem. Photobiol. C, 2011, 12, 20-30.
19 E. V. Kuzmenkina, C. D. Heyes and G. U. Nienhaus, Proc. Natl. Acad. Sci. U.S.A., 2005, 102, 15471-15476.
20 H. Chen, S. Kim, W. He, H. Wang, P. S. Low, K. Park and J.-X. Cheng, Langmuir, 2008, 24, 5213-5217.
21 M. You, E. Li, W. C. Wimley and K. Hristova, Anal. Biochem., 2005, 340, 154-164.
22 D. Nettels, I. V. Gopich, A. Hoffmann and B. Schuler, Proc. Natl. Acad. Sci. U.S.A., 2007, 104, 2655-2660.
23 J. N. Miller, Analyst, 2005, 130, 265-270.
24 T. Swift, J. Lapworth, K. Swindells, L. Swanson and S. Rimmer, RSC Adv., 2016, 6, 71345-71350.
25 T. Swift, N. Paul, L. Swanson, M. Katsikogianni and S. Rimmer, Polymer, 2017, 123, 10-20.
26 C. Li, J. Hu and S. Liu, Soft Matter, 2012, 8, 7096-7102.
27 G. Liu, J. E. Guillet, E. T. B. Al-Takrity, A. D. Jenkins and D. R. M. Walton, Macromolecules, 1991, 24, 68-74.
28 J. Wang, T. Yin, F. Huang, Y. Song, Y. An, Z. Zhang and L. Shi, ACS Appl. Mater., 2015, 7, 10238-10249.
29 N. Hao, C. Sun, Z. Wu, L. Xu, W. Gao, J. Cao, L. Li and B. He, Bioconjugate Chem., 2017, 28, 1944-1954.
30 M. A. Winnik and A. M. Sinclair, Macromolecules, 1985, 18, 1517-1518.
31 S. Ni, D. Juhue, J. Moselhy, Y. Wang and M. A. Winnik, Macromolecules, 1992, 25, 496-498.
32 Y. Sha, Q. Zhu, Y. Wan, L. Li, X. Wang, G. Xue and D. Zhou, J. Polym. Sci., Part A: Polym. Chem., 2016, 54, 2413-2420.
33 A. M. Breul, M. D. Hager and U. S. Schubert, Chem. Soc. Rev., 2013, 42, 5366-5407.
34 L. Qin, L. Li, Y. Sha, Z. Wang, D. Zhou, W. Chen and G. Xue, Polymers, 2018, 10, 1007.
35 D. A. Tomalia and D. P. Sheetz, J. Polym. Sci., Part A: Polym. Chem., 1966, 4, 2253-2265.
36 W. Seeliger, E. Aufderhaar, W. Diepers, R. Feinauer, R. Nehring, W. Thier and H. Hellmann, Angew. Chem. Int. Ed., 1966, 5, 875-888.
37 T. G. Bassiri, A. Levy and M. Litt, J. Polym. Sci. Pol. Phys., 1967, 5, 871-879.
38 T. Kagiya, S. Narisawa, T. Maeda and K. Fukui, J. Polym. Sci. Pol. Phys., 1966, 4, 441-445.
39 B. Verbraeken, B. D. Monnery, K. Lava and R. Hoogenboom, Eur. Polym. J., 2017, 88, 451-469.
40 E. Rossegger, V. Schenk and F. Wiesbrock, Polymers, 2013, 5.
41 B. A. Drain and C. R. Becer, Eur. Polym. J., 2019, 119, 344-351.
42 T. Lorson, M. M. Lübtow, E. Wegener, M. S. Haider, S. Borova, D. Nahm, R. Jordan, M. Sokolski-Papkov, A. V. Kabanov and R. Luxenhofer, Biomaterials, 2018, 178, 204-280.
43 L. Benski and J. C. Tiller, Eur. Polym. J., 2019, 120, 109233.
44 E. Cagli, E. Ugur, S. Ulusan, S. Banerjee and I. Erel-Goktepe, Eur. Polym. J., 2019, 114, 452-463.
45 J.-R. Park, J. F. R. Van Guyse, A. Podevyn, E. C. L. Bolle, N. Bock, E. Linde, M. Celina, R. Hoogenboom and T. R. Dargaville, Eur. Polym. J., 2019, 120, 109217.
46 V. V. Jerca, F. A. Nicolescu, D. S. Vasilescu and D. M. Vuluga, Polym. Bull., 2011, 66, 785-796.
47 S. Nam, J. Seo, S. Woo, W. H. Kim, H. Kim, D. D. C. Bradley and Y. Kim, Nat. Commun., 2015, 6, 8929.
48 J.-H. Kim, Y. Jung, D. Lee and W.-D. Jang, Adv. Mater., 2016, 28, 3499-3503.
49 M. Hartlieb, T. Bus, J. Kübel, D. Pretzel, S. Hoeppener, M. N. Leiske, K. Kempe, B. Dietzek and U. S. Schubert, Bioconjugate Chem., 2017, 28, 1229-1235.
50 J.-H. Kim, D. Yim and W.-D. Jang, Chem. Commun., 2016, 52, 4152-4155.
51 S. Nam, V. R. d. l. Rosa, Y. Cho, R. Hamilton, S. Cha, R. Hoogenboom and D. D. C. Bradley, Appl. Phys. Lett., 2019, 115, 143302.
52 S. W. Hong, K. H. Kim, J. Huh, C.-H. Ahn and W. H. Jo, Chem. Mater., 2005, 17, 6213-6215.
53 M. A. Hossain, H. Mihara and A. Ueno, J. Am. Chem. Soc., 2003, 125, 11178-11179.
54 M. M. Lübtow, L. C. Nelke, J. Seifert, J. Kühnemundt, G. Sahay, G. Dandekar, S. L. Nietzer and R. Luxenhofer, J. Controlled Release, 2019, 303, 162-180.
55 L. Hahn, M. M. Lübtow, T. Lorson, F. Schmitt, A. Appelt-Menzel, R. Schobert and R. Luxenhofer, Biomacromolecules, 2018, 19, 3119-3128.
56 M. M. Lübtow, L. Hahn, M. S. Haider and R. Luxenhofer, J. Am. Chem. Soc., 2017, 139, 10980-10983.
57 O. Sedlacek and R. Hoogenboom, Advanced Therapeutics, 2020, 3, 1900168.

58 T. Swift, R. Hoskins, R. Telford, R. Plenderleith, D. Pownall and S. Rimmer, J. Chromatogr. A, 2017, 1508, 16-23.
59 W. H. Melhuish, J. Phys. Chem., 1961, 65, 229-235.
60 R. Hoogenboom, M. W. M. Fijten, C. Brändli, J. Schroer and U. S. Schubert, Macromol. Rapid Commun., 2003, 24, 98-103.
61 D. C. Dong and M. A. Winnik, Photochem. Photobiol., 1982, 35, 17-21.
62 M. S. A. Abdel-Mottaleb, M. S. Antonious, M. M. Abo-Aly, L. F. M. Ismaiel, B. A. El-Sayed and A. M. K. Sherief, J. Photochem. Photobiol., A, 1989, 50, 259-273.
63 S. Huber, N. Hutter and R. Jordan, Colloid. Polym. Sci., 2008, 286, 1653-1661.
64 I. Z. Steinberg, The Journal of Chemical Physics, 1968, 48, 2411-2413.
65 N. Felorzabihi, P. Froimowicz, J. C. Haley, G. R. Bardajee, B. Li, E. Bovero, F. C. J. M. van Veggel and M. A. Winnik, The Journal of Physical Chemistry B, 2009, 113, 2262-2272.
66 B. Stubbe, Y. Li, M. Vergaelen, S. Van Vlierberghe, P. Dubruel, K. De Clerck and R. Hoogenboom, Eur. Polym. J., 2017, 88, 724-732.

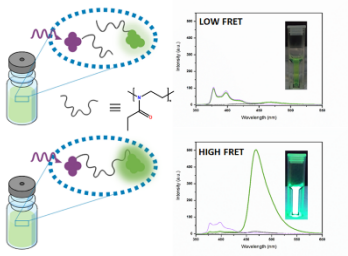

A well-defined FRET system based on heterotelechelic poly(2-ethyl-2-oxazoline) containing pyrene and coumarin 343 was successfully used as fluorescent probe for temperature sensing, while in the solid state (e.g., fibers and films) the polymers showed excellent FRET efficiency being promising candidates for solar cells and/or bioimaging.